Growth Characteristics of Nano-grained Sm-doped Ceria Film Prepared by E-beam Evaporation

Hong-Hsin Huang[1 *], Hung-Peng Chang[2], Moo-Chin Wang[3], I-Ming Hon[4], Fang-Hsing Wang[2], Kuan-Zong Fung[4]

[1]Department of Electrical Engineering, Cheng Shiu University, 840, Cheng Ching Rd., Niaosong, Kaohsiung, 83347, Taiwan

[2]Department and Institute of Electrical Engineering, National Chung-Hsing University, 250, Kuo Kuang Rd., Taichung, Taiwan

[3]Department of Mechanical Engineering, National Kaohsiung University of Applied Sciences, 415, Chien-Kung Road, Kaohsiung, 80782, Taiwan

[4]Department of Materials Science and Engineering, National Cheng Kung University, 1, Ta-Hsueh Road, Tainan, 70101, Taiwan

Corresponding author: E-Mail funs@csu.edu.tw

TEL +886-7-7310606 ext.3409, FAX +886-7-7337390

Abstract

Sm-doped Ceria (SDC) film with nano-pyramidal or triangular terrace morphology is prepared by E-beam evaporation at low temperature. Preferred orientation of SDC films transfers from [111] to [220] with the film thickness increasing. Texture coefficient of reflections clearly shows the trend and it is as high as 2.4 when film thickness is 1200 nm. A nano-pyramidal morphology is found when film thickness is 100 nm, however, a triangular terrace morphology is found when film thickness is higher. The layers of triangular terrace are clearly found because of continuous nucleation and growth from a nano-pyramidal grain simultaneously. According to cross section observation, the (111) plane possessing lowest surface energy grows resulting in the triangular terrace and the preferred orientation of (220) for high film thickness. The result of TEM analysis agrees with this phenomenon.

Keyword: E-beam evaporation, nano-pyramidal morphology, preferred orientation, triangular terrace morphology

PACS codes: 68.55.Jk, 81.07.Bc, 81.15.Jj, 68.47.Gh

1. Introduction

By doping with aliovalent cation (trivalent or divalent), oxygen vacancies are created in the ceria lattice for charge compensation, which may be prepared to give electronic, ionic and mixed modes of conductivity. They are valuable for a variety of applications, such as oxygen-ion conducting electrolytes in solid oxide full cells (SOFCs) operating at intermediate temperature (400-700 °C) [1].

SDC thin films may be prepared by a variety of processing techniques, such as, off-axis RF sputtering [2], metal-organic chemical vapor deposition (MOCVD) [3], molecular beam epitaxy [4], E-beam evaporation [5], thermal evaporation [6], and spray pyrolysis [7]. Significantly, E-beam evaporation offers two major advantages: (1) a high power density, and hence a wide range of control over evaporation rates, from very low to very high and (2) the source material for evaporation being contained in the water-cooled crucible and its surface area showing a high temperature. Metallurgical reactions between crucible and source materials leading to film contamination are therefore minimized.

Ceria with a fluorite structure is supposed to be an ideal buffer layer for fabricating epitaxial perovskite materials on silicon substrates because of its excellent lattice match with Si. Preparation of ceria (100) film is more attractive for applications compared to that of (111). Ceria (100) films could be deposited by

E-beam assisted evaporation at 750 °C [9], by off-axis RF sputtering at 640-800 °C [2], by metalorganic chemical vapor deposition (MOCVD) at 600-900 °C [10,11], and by combustion chemical vapor deposition at 1000 °C [12]. The excellent epitaxy of ceria films was achieved on a (111) Si substrate without any amorphous layer in the vicinity of the boundary by pulsed laser deposition in an ultrahigh vacuum at room temperature [13]. However, the preferred orientation of ceria on (100) Si substrates reported was not ceria (100) but (110) [14,15]. The epitaxial ceria (110) layers grown on Si(100) substrates at low temperature had also reported by Inoue et al. [16]. Thus, the preferred orientation of ceria films is determined by prepared method, deposition parameters and substrate.

In general, thin film growth needs enough migration energy for absorbed atoms and/or molecules. In order to lower the deposition temperature, the electron beam assisted evaporation had been used by Inoue et al. [16] to lower the epitaxial growth temperature to 710 °C, where electron beams irradiated on to the substrate surface simultaneously with evaporation. The growth behavior of ceria on Si(111) and Si(100) have been reported by Inoue et al. [14,16] at temperature higher than 710 °C by using electron beam assisted evaporation technique. However, the SDC thin films prepared by electron beam evaporation at temperature less than 200 °C without extrinsic assistance have not been conducted.

In the present investigation, the nano-grained SDC films have been prepared by E-beam evaporation on Si(100) substrate at low temperature of 150 °C. The growth characteristics such as thickness-dependent texture and morphology of SDC films are discussed in detail.

2. Experimental

SDC powder, to be used as the source material for E-beam evaporation, was formed and sintered at 1400 °C for 4 h. The silicon (100) substrate was cleaned in isopropyl alcohol (EPA) and deionized water and dried by nitrogen gas. For deposition, substrates were fastened in a curved holder with a working distance of 20 cm. A diffusion-pumped vacuum system with a base pressure of 5×10^{-6} Torr was used for deposition. Oxygen was introduced into the chamber to adjust the working pressure. Substrate temperature was kept at 150 °C. The deposition rate of SDC was controlled by an E-beam power and monitored by a thickness control system (CRTM-6000, ULVAC, Japan) and various film thicknesses, namely 100, 300, 900 and 1200 nm, were obtained. The structure of SDC films were identified by XRD with Cu Kα radiation and a Ni filter, operated at 30 kV, 30 mA, a scanning rate of 4 °/min and 2θ of 20° - 80° (MAX 2500, RIGAKU). The morphology of the SDC films was observed by SEM (S4800, HITACHI, Japan). The microstructure of the SDC

films was analyzed by TEM (Tecnai G^2, FEI, Netherlands, Czech).

3. Results and discussion

The structure of SDC films prepared by E-beam evaporation with various thicknesses is analyzed by XRD and shown in Fig.1. The diffraction peaks of (111), (220), (311), (400), (331) and (420) planes of polycrystalline SDC are found. For ceria (111) surface, all exposed Ce ions are seven-coordinated and all surface O ions are bonded to three Ce ions, which possess the smallest surface energy, followed by (110). Fig.1 (a) shows the XRD pattern of the SDC film with a thickness of 100 nm where the highest intensity is (111), followed by (220). It reveals that the surface energy dominated in the nucleation and initial growth region. As film thickness increasing, the (220) possess the highest intensity in Fig.1 (d) meaning that the preferred orientation of SDC films grown in this situation is not (111) but (220).

In Fig.1, the intensity of (220) increases with the film thickness, however, the intensity of (111) trends to disappear. Sakamoto et al. [9] reported that the CeO_2 films prepared by E-beam assisted evaporation at room temperature possess the texture of (111), however, a low intensity of (220) is found in the XRD pattern. The intensity of (220) is highest when the films deposited at higher temperatures of 200 and 400 °C. Nevertheless, Toro et al. [11] reported that a (002) ceria film deposited by MOCVD at

600 °C, a (111) ceria film deposited at higher temperature of 900 °C on a (001) TiO_2 substrate. From Fig.1, these results agree with that of Inoue et al. [16] where the preferred orientation of SDC deposited on Si(100) is [220].

The preferred orientation of a film is usually found and can be evaluated by texture coefficient, TC [17]. Fig.2 shows the dependence of TC values on film thickness. For films thickness less than 300 nm, the preferred orientation of SDC is [111], however, the preferred orientation changes to [110] when the film thickness is higher than 300 nm. It is found that the TC values level off with the thickness increasing, which reveals that the preferred orientation is [110] in this deposition condition. The preferred orientation of thin films is considerably determined by prepared method, deposition parameters and substrate. The dependence of preferred orientation of ceria films on deposition temperature had been reported by Sakamoto et al. [9], nevertheless, the effect of thickness on preferred orientation is not discussed simultaneously. Fig.2 reveals that the thickness of 300 nm is a critical thickness to obtain the preferred orientation of SDC films deposited by E-beam evaporation at 150 °C. The thickness-dependent preferred orientation of TiN thin films had been reported by Oh et al. [18], and they showed the strong dependence of the change in preferred orientation on strain energy in TiN thin films.

The morphology of the SDC films is observed by SEM and shown in Fig.3. In

Fig.3(a) reveals that more nano-pyramidal particles is found on the surface when film thickness is 100 nm, whereas, the triangular grained morphology is found when the film thickness is 1200 nm as shown in Fig.3 (b). When film thickness is low there are a lot of nano-pyramidal grains observed meaning that the nucleation behavior dominated. Nevertheless, there is less nucleation grain found in Fig.3 (b), but big triangular grains are found meaning that the grain growth dominated when the film thickness is high. A morphology of gable-roof-shaped stripes of ceria thin film prepared by E-beam assisted evaporation is found and the preferred orientation of [110] consisting of a pair of (111) facets [16]. The morphology of nanostrips also reported by Nörenberg and Briggs [19] who observed the morphology of ceria annealed at high temperature. From Fig.3, the (111) facetted SDC grains grew with an angle could be deduced.

The cross section observation of SDC film is observed by SEM and shown in Fig.4 which reveals that the layer structure is found followed a columnar growth. According to Fig.3(b), the triangular grains nucleated in the center and grew laterally to form the layer structure. The lateral growth with a similar thickness is found which reveals that the nucleation and growth happen simultaneously. On the other hand, the lateral growth was obstructed when these grains touched each others to form a columnar structure perpendicular to the substrate as shown in Fig.4. For a fluorite

structure, it is deduced that the angle between the {110} and [110] is similar to that observed in Fig.4.

The TEM analysis of (a) bright field, (b) dark field and (c) selected area electron diffraction pattern of SDC films are shown in Fig.5. The nano-grains of SDC films are found in Figs.5 (a) and (b), however, there are no triangular grain as seen in Fig.3 is found meaning that the three corners of the triangular grain did not locate within a horizontal plane. The lattice parameter can be measured from the rings of a selected-area electron diffraction pattern from many grains. As shown in Fig.5 (c), the lattice constant of the nano-grains is 0.545 nm.

Fig.6 shows the HR-TEM analysis of the SDC film, which indicates that the crystallites are oriented along the [110] crystallographic direction. Ceria nanoparticles with the [110] crystallographic direction had been prepared by Aneggi et al. [20] and they deduced that the dominant lattice fringes in all cases correspond to the {111} family. Inoue et al. [16] had reported the results of XTEM analysis of ceria indicating that the surface of the (110)-plane-cross-section of gable-roof shaped grain proved to consist of two (111) facets. According to Figs.3 and 4, the SDC crystallites probably grow by minimizing the surface energy with the formation of a lattice-matched coherent interface [21], which may explain the observed distribution of crystallites with a preferred orientation of [110].

4. Conclusion

The thickness-dependent texture and morphology of SDC films prepared by E-beam evaporation at 150 °C are found. The preferred orientation of SDC films transfer from [111] to [110] with the thickness increasing, moreover, a critical thickness of 300 nm is obtained according to the TC value calculation. The nano-pyramidal morphology is found when the thickness of the SDC film is 100 nm, however, the triangular terrace morphology is obtained when the film thickness is 1200 nm. For cross section observation, the terraces possessing layer structure with similar thickness are found because the nucleation and lateral grain growth happen simultaneously. On the other hand, the growth of the terraces maintains a angle with the substrate.

Acknowledgments

This work was supported by the National Science Council (Taiwan, The Republic of China under Contract No. Nsc 92-2216-E-230-002. The authors sincerely thank Mr. J.M. Chen and Prof. G.-J. Chen for assistance in XRD and TEM.

Reference

[1] J.-G. Li, T. Ikegami, T. Mori, Acta Materials 52 (2004) 2221.

[2] M. Španková, I. Vávra, S. Gaži, D. Machajdík, S. Chromik, K. Fröhlich, L. Hellemans, Š. Beňačka, J. Cryst. Grow. 218 (2000) 287.

[3] T. Ami, M. Suzuki, Mat. Sci. Eng. B 54 (1998) 84.

[4] M. Yoshimoto, K. Shimozono, T. Maeda, T. Ohnishi, M. Kumagai, T. Chikyow, O. Ishiyama, O. Shinohara, H. Koimuma, Jpn. J. Appl. Phys. 34 (1995) L688.

[5] C.-Y. Yang, S.E. Babcock, A. Goyal, M. Paranthaman, F.A. List, D.P. Norton, D.M. Kroeger, A. Ichinose, Physica C, 307 (1998) 87.

[6] G. Hass, J.B. Ramsey, R. Thun, J. Opt. Soc. Am. 48 (1958) 324.

[7] K. Konstantinov, I. Stambolova, P. Peshev, B. Darriet, S. Vassilev, Intl. J. Inorg. Mat. 2 (2000) 277.

[8] X. Hou, K.-L. Choy, Surf. Coat. Technol. 180-181 (2004) 15.

[9] N. Sakamoto, T. Inoue, K. Kato, Crystal Growth & Design 3(2) (2003) 115.

[10] R. L. Nigro, G. Malandrino, I. L. Fragala, Chem. Mater. 13 (2001) 4402.

[11] R.G. Toro, G. Malandrino, I.L. Fragala, R.L. Nigro, M. Losurdo, G. Bruno, J. Phys. Chem. B 108 (2004) 16357.

[12] W.B. Carter, G.W. Book, T.A. Polley, D.W. Stollberg, J.M. Hampikian, Thin Solid Films 347 (1999) 25.

[13] M. Yoshimoto, K. Shimozono, T. Meada, Jpn. J. Appl. Phys. 35 (1995) 688.

[14] T. Inoue, Y. Yamamoto, S. Suzuki, Y. Ueda, Appl. Phys. Lett. 56 (1990) 1332.

[15] T.S. Chin J.Y. Huang, L.H. Perng, T.W. Huang, S.J. Yang, S.E. Hsu, Phys. C 192 (1992) 1332.

[16] T. Inoue, S. Shida, N. Yakamoto, A. Horikawa, M. Ohashi, J. Cryst. Grow. 253 (2003) 366.

[17] H. H. Huang, M. H. Hon, Thin Solid Films 416 (2002) 54.

[18] U.C. Oh, H. Je, J.Y. Lee, J. Mat. Res. 13 (1998) 1225.

[19] H. Nörenberg and G.A.D. Briggs, Surf. Sci. 433-435 (1999) 127.

[20] E. Aneggi, J. Liorca, M. Boaro, A. Trovareli, J. Catal. 234 (2005) 88.

[21] Z.I. Wang, X. Feng, J. Phys. Chem. B 107 (2003) 13563.

Figure captions

Fig.1 XRD patterns of SDC films with various thicknesses of (a) 100, (b) 300, (c) 900 and (d) 1200 nm.

Fig.2 Dependence of texture coefficients of SDC films on thickness.

Fig.3 Morphology of SDC films with thickness of (a) 100 and (b) 1200 nm.

Fig.4 A cross section SEM micrograph of a 1200 nm thick SDC film.

Fig.5 (a) Bright field images, (b) dark field images and (c) selected-area diffraction pattern of SDC film.

Fig.6 HR-TEM analysis of SDC film.

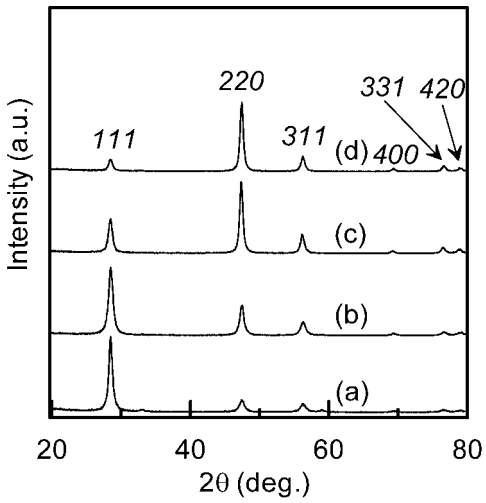

Fig.1

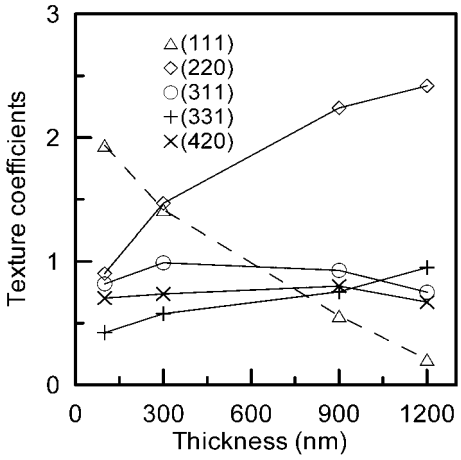

Fig.2

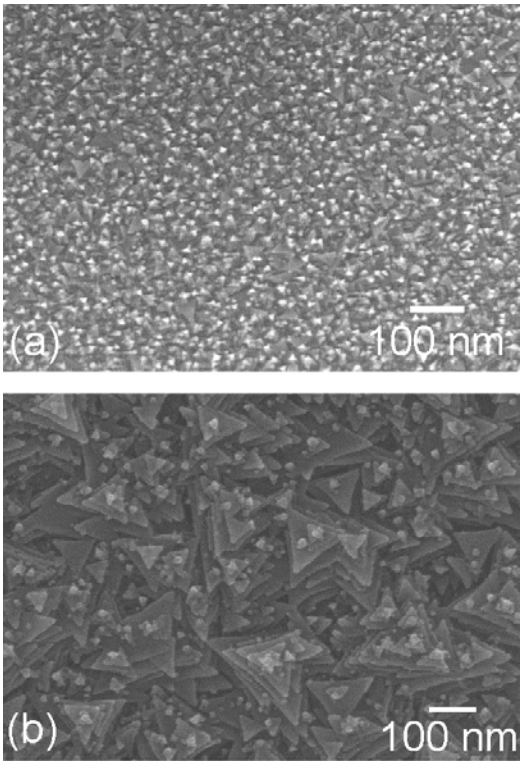

Fig.3

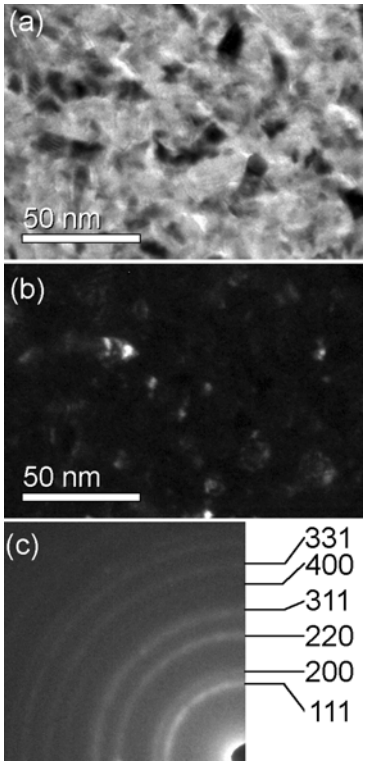

Fig.5

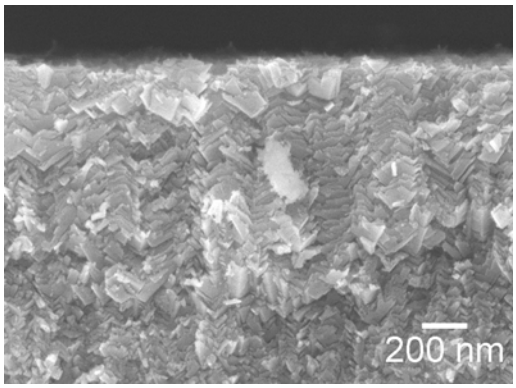

Fig.4

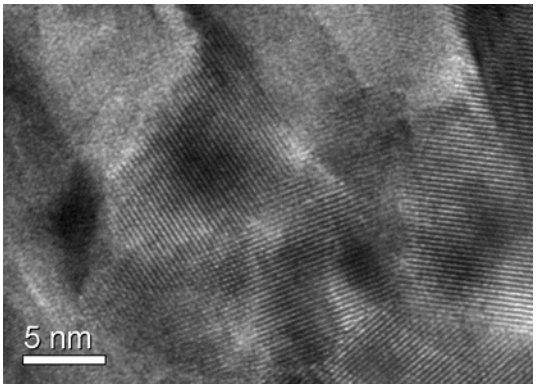

Fig.6